Neutron capture cross sections of ^{148}Gd and the decay of ^{149}Gd

M. G. Rios,[1,*] R. J. Casperson,[1,†] K. S. Krane,[1] and E. B. Norman[2,‡]
[1]*Department of Physics, Oregon State University, Corvallis, Oregon 97331, USA*
[2]*Nuclear Science Division, Lawrence Berkeley Laboratory, Berkeley, California 94720, USA*
(Received 12 September 2005; published 4 October 2006)

The thermal cross section and resonance integral were measured for radiative neutron capture by radioactive ^{148}Gd. The deduced values are $\sigma = 9600 \pm 900$ b and $I = 28,200 \pm 2300$. We also deduced upper limits for the n,p and n, α cross sections, respectively, 0.25 b and 13 b. The γ-ray spectrum from the decay of ^{149}Gd was studied in singles mode at high resolution to verify the previously determined energies and intensities. From the latter measurements, new transitions are proposed and upper limits are deduced for previously reported transitions.

DOI: 10.1103/PhysRevC.74.044302 PACS number(s): 21.10.−k, 23.20.Lv, 25.40.Lw, 27.60.+j

I. INTRODUCTION

The odd-mass Gd isotopes ($A = 153, 155, 157, 161$) are known to have large cross sections for radiative thermal neutron capture, in the range of 30,000–250,000 b [1]. By contrast, the thermal cross sections of the even-mass Gd isotopes ($A = 152$, 154, 156, 158, 160) are significantly smaller, typically 1–1000 b. No similar systematic behavior is seen in the other elements in this region (Sm, Eu, Tb, Dy). To extend the knowledge of cross sections in this region, we measured the thermal capture cross section and resonance integral of ^{148}Gd. Preliminary reports of these results have been previously presented [2,3].

In the process of analyzing the γ rays from the decay of ^{149}Gd to determine the cross sections, some inconsistencies in the previously determined γ-ray intensities became apparent. Previous studies of this decay used sources produced by spallation or heavy-ion reactions; no previous report exists of the decay of a ^{149}Gd sample produced through neutron capture by ^{148}Gd. We therefore include in this work a detailed study of the singles-mode decay of ^{149}Gd at high resolution, and we report here our determination of the energies and intensities of the γ rays.

II. EXPERIMENTAL DETAILS

A. Cross sections

Radioactive source material of ^{148}Gd (a pure α emitter with a half-life of 75 yr) was obtained from two suppliers: Los Alamos National Laboratory [4] and Isotope Products Laboratory [5]. Both samples were in the form of a dilute HCl solution. For the cross section measurements, small quantities of the liquid were sealed in either polyethylene vials or quartz ampoules for irradiation. In some cases the liquid was evaporated to dryness prior to irradiation and then taken up with fresh HCl after irradiation.

The irradiations were performed in the TRIGA reactor at Oregon State University. Three different irradiation facilities were used: an in-core irradiation tube (ICIT); a cadmium-lined in-core irradiation tube (CLICIT), with a negligible thermal flux (below a cutoff of 0.5 eV) and the same epithermal flux as the ICIT; and a thermal column (TC). Measured flux values in these facilities are given in Table I. Irradiations typically lasted from one to several hours.

Following the irradiations, the samples were diluted with pure water in a ratio from 3:1 to 10:1, and a small amount of the liquid was dried on a piece of aluminized Mylar. The dried spot size was typically about 4–7 mm in diameter. These samples were counted by first using a particle detector to determine their ^{148}Gd content from their α emissions and then using a γ-ray detector to determine their ^{149}Gd content.

The monoenergetic α emissions from ^{148}Gd (3.183 MeV) were counted in a vacuum chamber using a Si surface barrier detector 9 mm in diameter and 1 mm in thickness. The samples were placed at either 5 or 10 cm from the detector surface. The detector efficiency (due only to geometrical effects) was determined from a geometrical calculation and also by using a calibrated ^{241}Am source. The α activity of the samples was used to deduce their ^{148}Gd content. The α counting generally lasted from several hours to a full day. A sample α spectrum is shown in Fig. 1.

The γ rays were counted using a high purity Ge (HPGe) detector connected to a digital spectroscopy system. The detector had an active volume of 169 cm^3 and a resolution of 1.65 keV for the 1.33-MeV γ ray of ^{60}Co (with an efficiency of 35% compared with NaI). Because the samples were very weak, small source-to-detector distances were used (either 5 or 7.5 cm). Even so, the count rates were quite small, as low as 0.01–0.03 counts/s for the strongest γ rays. For our determination of the activities, we used the three most intense transitions: 150 keV (48.2%), 299 keV (28.6%), and 347 keV (23.9%) [6]. The samples were counted for several days to obtain good statistics for determining the activities.

For the determination of the neutron fluxes, we used a variety of flux monitors: ^{59}Co and ^{197}Au in dilute Al alloys served as primary flux monitors, and ^{58}Fe, ^{64}Zn, and ^{94,96}Zr were used as secondary flux monitors. All flux monitors were in the form of thin metal foils of natural isotopic abundances

*Present address: Advanstar Communications, Eugene, OR 99401.
†Present address: Department of Physics, Yale University, New Haven, CT 06520-8120.
‡Present address: Lawrence Livermore National Laboratory, Livermore, CA 94550.

TABLE I. Summary of irradiation parameters of ^{148}Gd cross section determinations.

Irradiation number	Irrad. time (h)	Sample number	^{148}Gd activity (Bq)	^{149}Gd EOB activity (Bq)	Neutron flux ($\times 10^{10}$ n/cm^2/s)		σ ($\times 10^3$ b)	I ($\times 10^3$ b)
					Thermal	Epithermal		
CLICIT 1	1	A	6.03(6)	2.41(20)	—	119		26.9
		B	19.7(1)	8.43(24)	—	119		29.6
TC 2	4	A	429(11)	12.6(13)	6.3	0.02	10.1	
		B	170(1)	4.33(24)	6.3	0.02	9.53	
TC 3	3	A	378(1)	9.96(20)	6.7	0.02	9.35	
		B	269(1)	7.18(25)	6.7	0.02	9.49	
		C	670(2)	18.45(31)	6.7	0.02	9.78	
ICIT 4	4	A	244(5)	3150(63)	900	200	10.8	
		B	186(4)	2510(50)	900	200	11.2	
ICIT 5	1	A	8.13(7)	8.97(37)	820	119	7.99	
		B	8.50(7)	9.38(38)	820	119	8.17	
		C	20.2(1)	24.38(50)	820	119	9.39	

and were irradiated simultaneously with the ^{148}Gd. In effect, our determinations of the thermal cross sections and resonance integrals of ^{148}Gd are carried out by comparison with the accepted values of the thermal cross sections and resonance integrals of these standards. The use of these reference standards is discussed in a previous publication [7].

Energies and intensities were determined from the spectra using the code MAESTRO [8]. The peak areas were determined by summing the counts above a linear background. These results were checked against a more detailed peak fitting routine (SAMPO [9]) and found to be identical (within statistical uncertainties) for the three peaks used in the cross section determinations.

B. γ-Ray spectroscopy

For the spectroscopic studies of the ^{149}Gd decay, three different samples were prepared by irradiating quantities of ^{148}Gd activity each approximately 10^3 times stronger than was used for the cross section determinations. The resulting samples of ^{149}Gd in HCl solution were counted in cylindrical vials approximately 6 mm in diameter and 10 mm in height.

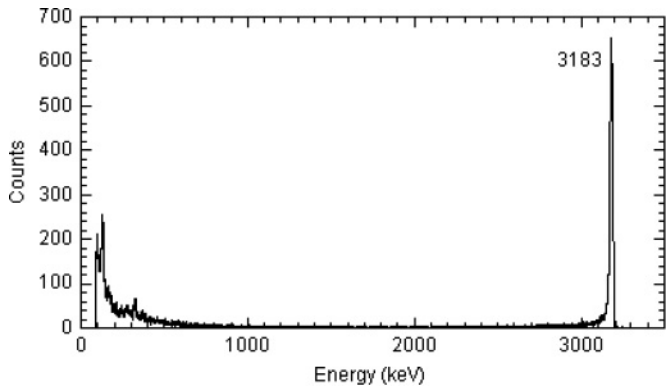

FIG. 1. The α spectrum from the decay of ^{148}Gd.

The first sample had an initial activity of 84 kBq and was counted at 12 cm from a HPGe detector for 3.5 days. The second sample had an initial activity of 10.5 kBq and was counted for 9 days at 20 cm and then for another 9 days at 15 cm. The third sample had an initial activity of 38 kBq and was counted at 7.5 cm for 9 days and then at 5 cm for 9 days. The peak centroids and areas were determined using the code SAMPO. The energies and intensities were obtained by fitting each of these five spectra separately, and then the five results for each peak were averaged together.

Efficiency calibration of the detectors was carried out using National Institute of Standards and Technology (NIST)-traceable calibrated sources of ^{133}Ba and ^{152}Eu. Owing to the difficulty of extending the efficiency calibration below 200 keV (where the dependence of the efficiency on energy deviates from the simple power-law dependence that characterizes the behavior above 200 keV), special care was taken to check the efficiency calibrations against accepted γ-ray intensities from sources that have strong γ emissions both above and below 200 keV. For this purpose, we produced sources of ^{160}Tb, ^{169}Yb, and ^{182}Ta by neutron irradiation. The analysis of the γ-ray intensities from these sources using our efficiency calibrations gave results that agreed with the accepted relative intensities in the low-energy region to within 2–3%, which we believe to be a reasonable limit on the uncertainties that can be obtained from these studies. Indeed, Debertin and Helmer [10] assert that the best achievable uncertainty in efficiency under optimal conditions is perhaps 0.5% in the region above 120 keV and no better than 1% in the low-energy region where the efficiency curve "turns over." We take a slightly more conservative view and assume that the efficiency calibration process sets a limit on the intensity precision corresponding to an uncertainty of 2% below 200 keV and 1% above 200 keV. The peak fitting process (especially for unresolved multiplets) and the statistical uncertainties of weak peaks can of course increase these limits. Furthermore, we treat the calibration uncertainties as systematic and therefore as not reducible by averaging results from multiple experiments.

III. RESULTS

A. Cross sections

Ultimately the determination of the ^{148}Gd cross sections requires a measurement of the ratio of the activities of ^{149}Gd and ^{148}Gd in each sample. The ^{149}Gd activity is produced in the reactor at a rate given by $N_{148}\sum\sigma_i\phi_i$, where N_{148} is the number of ^{148}Gd atoms (which we assume to be constant during the time of the irradiation because of the long half-life of ^{148}Gd). The sum of the product of the cross section σ_i and the neutron flux ϕ_i is carried out over all relevant regions of the neutron spectrum that can contribute to the activation. In our case the only important contributions come from the thermal region (where we represent the effective cross section as σ and the flux as ϕ_{th}) and the epithermal region (where the cross section is represented by the resonance integral I and the flux is ϕ_{epi}). This analysis is dependent in part on the assumption that the cross section far from the resonance region depends on the neutron speed v as v^{-1}; this is equivalent to assuming that there are no broad or low-lying resonances or that the Westcott g factor is equal to unity [1]. The resonance structure of ^{148}Gd is not known, but our results give identical values for the effective thermal cross section using neutrons with a thermal spectrum and with unthermalized neutrons in the reactor core, which supports the assumption of a v^{-1} cross section. With $N_{148} = a_{148}/\lambda_{148}$ (where a is the activity and λ is the decay constant), we can then represent the rate of ^{149}Gd production as $(a_{148}/\lambda_{148})(\sigma\phi_{\text{th}} + I\phi_{\text{epi}})$. The activity of ^{149}Gd at the end of bombardment time t_b can then be found by solving the rate equation, which then gives

$$\sigma\phi_{\text{th}} + I\phi_{\text{epi}} = \frac{a_{149}}{a_{148}}\frac{\lambda_{148}}{(1 - e^{-\lambda_{149}t_b})}. \quad (1)$$

We performed a total of five irradiations: two in the TC (from which five samples were prepared and counted), two in the ICIT (five samples), and one in the CLICIT (two samples). We prepared multiple samples from each irradiation to verify the uniformity of the source material. Each sample was counted first in the α spectrometer, next with the γ counter, and then again with the α counter to verify that no activity had been lost between the α and γ counting.

Table I shows a summary of the cross section measurements. From the CLICIT runs, the ^{148}Gd resonance integral is determined to be

$$I = 28,200 \pm 2300\,\text{b}.$$

The uncertainty in this value is due primarily to the range of values of the epithermal flux as determined from the various flux monitors (±4%) but also includes a contribution from the uncertainties in the efficiency of the γ-ray detector (±2%) and the α-particle detector (±2%). A net uncertainty of ±8% is representative of all such contributions.

The TC runs yielded a value of the thermal cross section of $\sigma = 9600 \pm 900$ b, with an uncertainty deduced in a manner similar to that of the resonance integral. The ICIT data depend on both the thermal cross section and the resonance integral. Based on the values deduced so far for these parameters and the roughly 5:1 ratio of the thermal and epithermal fluxes in the ICIT, we expect that the ICIT data are about a factor of 2 more sensitive to the thermal cross section than to the resonance integral. We have therefore chosen to analyze the ICIT data by assuming the above value for the resonance integral obtained from the CLICIT data and solving for the value of the thermal cross section, which gives $\sigma = 9500 \pm 1200$ b (the larger uncertainty here is in part due to the uncertainty in the resonance integral in addition to the systematic uncertainties discussed above). These two results for the thermal cross section are in good agreement, and we take their unweighted average as our best experimental value for the thermal cross section:

$$\sigma = 9600 \pm 900\,\text{b},$$

where the net uncertainty is taken as the smaller of the two individual values, because the primary contributions to the uncertainty are systematic rather than statistical. The good agreement between the effective thermal cross sections obtained in irradiation facilities with very different neutron energy distributions lends confidence to the validity of these results and justifies the implicit assumption in our analysis of the v^{-1} behavior of the cross section in the thermal region. The flux monitors are well known to exhibit v^{-1} behavior and have no low-energy or excessively broad resonances that distort the low-energy cross section (see Ref. [1]); thus the deduced thermal flux represents the effective 2200 m/s value. The agreement of the TC and ICIT thermal cross sections suggests that our deduced value represents the effective 2200 m/s cross section with negligible distortion from any possible non-v^{-1} effects.

We also examined our data for the presence of 54.5-d ^{148}Eu and 340-d ^{145}Sm, which can be produced from ^{148}Gd, respectively, through the n, p ($Q = -0.758$ MeV) and n, α ($Q = +9.246$ MeV) reactions. We observe no evidence for either of these activities in any of our samples. From the upper limit on the intensity of the 550-keV γ ray (98.5% branch) from ^{148}Eu, we conclude that

$$\sigma(\text{n, p}) < 0.25\,\text{b},$$

and from an upper limit on the 61-keV γ ray (12%) from ^{145}Sm, we conclude that

$$\sigma(\text{n}, \alpha) < 13\,\text{b}.$$

B. γ-Ray spectroscopy

Table II summarizes the results of the present spectroscopic study of the γ rays emitted following the decay of ^{149}Gd and compares our results with the presently accepted energies and intensities from the Nuclear Data Sheets (NDS) [11] and with the results of the two most precise recent studies reported by Adam *et al.* [12] and by Meyer [13]. (A more recent report by Cabrera *et al.* [14] is less complete and less precise than these two studies.)

In addition to the ^{149}Gd, immediately after the irradiation our samples contained about 0.7% ^{152}Eu, 0.1% ^{154}Eu, 2% ^{151}Gd, and 0.5% ^{153}Gd. These long-lived activities, which were produced by neutron activation of stable Eu and Gd present in our ^{148}Gd samples, did not interfere with the measurements of the ^{149}Gd γ rays; in fact they enhanced the experiment

TABLE II. Energies and intensities of γ rays emitted by ^{149}Gd determined in the present work compared with those of the Nuclear Data Sheets [11], Adam *et al*. [12], and Meyer [13].

NDS (2004)		Adam *et al*. (1987)		Meyer (1990)		Present work	
E	*I*	*E*	*I*	*E*	*I*	*E*	*I*
82.50 *15*	0.065 15					82.33 8	0.011 2
125.981 *10*	0.252 *7*	125.98 *2*	0.250 *7*	125.98 *1*	0.313 *10*	125.99 *2*	0.300 *6*
128.75 *3*	0.076 *5*	128.77 *11*	0.069 *7*	128.75 *3*	0.078 *5*	128.74 *2*	0.081 *7*
132.006 *9*	0.155 *8*	132.06 *3*	0.147 *6*	132.001 *9*	0.186 *10*	132.00 *1*	0.187 *11*
138.13 *5*	0.180 *7*	138.28 *4*	0.181 *7*	138.09 *2*	0.171 *15*	138.10 *1*	0.141 *8*
						139.74 *8*	0.029 *3*
149.735 *3*	100.0 *7*	149.740 *14*	100.0 *19*	149.736 *3*	100.0 *7*	149.72 *1*	100.0 *6*
184.512 *10*	0.097 *3*	184.52 *2*	0.099 *3*	184.51 *1*	0.093 *4*	184.50 *2*	0.108 *3*
186.74 *5*	0.0196 *16*	186.75 *7*	0.0192 *16*	186.729 *53*	0.0206 *25*	186.63 *3*	0.024 *4*
						213.39 *8*	0.009 *2*
214.277 *15*	0.403 *8*	214.268 *13*	0.409 *8*	214.28	0.387 *10*	214.28 *2*	0.409 *11*
252.219 *7*	0.561 *13*	252.203 *8*	0.580 *11*	252.222 *4*	0.538 *11*	252.19 *2*	0.563 *11*
260.736 *6*	2.74 *4*	260.735 *6*	2.69 *5*	260.737 *6*	2.69 *3*	260.73 *3*	2.69 *5*
264.67 *3*	0.086 *8*	264.72 *3*	0.095 *3*	264.63 *3*	0.064 *5*	264.60 *4*	0.081 *4*
266.97 *5*	0.063 *3*	266.97 *5*	0.063 *3*			266.82 *6*	0.036 *3*
272.321 *8*	6.67 *16*	272.322 *6*	6.69 *13*	272.317 *5*	6.66 *11*	272.32 *3*	6.61 *13*
278.28 *2*	0.144 *7*			278.28 *2*	0.143 *3*	278.34 *2*	0.185 *6*
298.634 *5*	59.4 *14*	298.634 *10*	57.9 *10*	298.634 *5*	57.7 *5*	298.63 *1*	57.9 *6*
						302.58 *3*	0.026 *4*
341.65 *5*	0.164 *11*	341.65 *5*	0.167 *11*	341.65 *6*	0.157 *15*	341.66 *5*	0.136 *17*
				346.30	0.15 *5*		
346.651 *3*	49.6 *7*	346.648 *5*	49.1 *8*	346.651 *3*	48.9 *4*	346.66 *3*	49.8 *5*
348.96 *10*	0.20 *5*			348.96 *10*	0.196 *49*	349.12 *10*	0.133 *10*
352.81 *2*	0.088 *6*	352.72 *9*	0.088 *6*	352.81 *2*	0.088 *15*	352.79 *5*	0.074 *9*
384.539 *10*	0.158 *5*	384.545 *12*	0.160 *4*	384.52 *2*	0.157 *5*	384.54 *2*	0.154 *4*
398.816 *12*	0.0926 *23*	398.82 *1*	0.0937 *23*	398.77 *3*	0.088 *5*	398.82 *3*	0.092 *3*
404.296 *5*	0.413 *6*	404.302 *9*	0.413 *6*	404.294 *5*	0.416 *10*	404.32 *3*	0.402 *5*
416.08 *3*	0.0487 *15*	416.11 *3*	0.0493 *15*	416.04 *3*	0.045 *4*	416.09 *4*	0.048 *3*
418.77 *13*	0.0108 *13*	418.77 *13*	0.0108 *13*			418.35 *4*	0.010 *2*
						419.47 *15*	0.006 *2*
421.63 *18*	0.0071 *11*	421.63 *18*	0.0071 *11*			421.55 *20*	0.010 *5*
431.297 *12*	0.148 *3*	431.298 *12*	0.147 *3*	431.294 *12*	0.142 *10*	431.30 *2*	0.145 *4*
436.369 *10*	0.098 *9*	436.37 *1*	0.132 *3*	436.36 *2*	0.132 *5*	436.24 *3*	0.091 *4*
436.369 *10*	0.033 *3*					436.62 *17*	0.043 *6*
456.78 *3*	0.0496 *24*	456.80 *3*	0.0506 *21*	456.75 *4*	0.044 *5*	456.74 *4*	0.048 *6*
459.814 *5*	1.202 *12*	459.821 *8*	1.222 *17*	459.812 *4*	1.199 *13*	459.84 *2*	1.224 *22*
478.29 *6*						478.27 *10*	0.047 *8*
478.710 *8*	0.472 *8*	478.710 *8*	0.473 *8*	478.71 *1*	0.475 *10*	478.78 *2*	0.424 *6*
482.635 *12*	0.153 *6*	482.636 *12*	0.155 *4*	482.63 *2*	0.157 *10*	482.66 *2*	0.155 *3*
492.81 *7*	0.0385 *25*	492.81 *7*	0.0385 *25*			492.93 *6*	0.034 *3*
496.383 *2*	3.44 *5*	496.380 *7*	3.41 *5*	496.383 *2*	3.43 *3*	496.41 *2*	3.35 *6*
516.545 *2*	5.59 *6*	516.549 *7*	5.60 *8*	516.545 *2*	5.53 *11*	516.57 *2*	5.58 *10*
534.295 *4*	6.37 *6*	534.288 *8*	6.5 *1*	534.296 *4*	6.41 *7*	534.31 *2*	6.49 *12*
552.760 *16*	0.179 *5*	552.768 *16*	0.181 *5*	552.75 *2*	0.171 *10*	552.76 *2*	0.156 *5*
563.48 *10*	0.0212 *22*	563.48 *10*	0.0212 *22*			563.58 *25*	0.024 *4*
598.94 *4*	0.0400 *21*	598.94 *4*	0.0400 *21*			598.84 *4*	0.047 *7*
601.201 *15*	0.122 *3*	601.196 *15*	0.1216 *26*	601.206	0.122 *5*	601.21 *3*	0.126 *7*
645.315 *2*	3.03 *2*	645.309 *7*	3.02 *4*	645.315 *2*	3.03 *3*	645.31 *1*	3.12 *4*
649.06 *8*	0.0223 *16*	649.06 *8*	0.0223 *16*			649.15 *7*	0.033 *4*
662.898 *15*	0.590 *10*	662.905 *10*	0.594 *11*	662.89 *1*	0.578 *11*	662.91 *1*	0.568 *10*
666.289 *4*	1.809 *13*	666.286 *7*	1.822 *28*	666.290 *4*	1.801 *16*	666.29 *1*	1.853 *22*
673.65 *15*	0.0067 *9*	673.65 *15*	0.0067 *9*			673.43 *2*	0.0076 *12*
726.21 *2*	0.170 *13*	726.21 *1*	0.162 *5*	726.16 *4*	0.166 *10*	726.23 *2*	0.168 *6*
734.863 *12*	0.262 *6*	734.87 *1*	0.261 *6*	734.84 *2*	0.274 *10*	734.85 *3*	0.262 *8*

TABLE II. *(Continued.)*

NDS (2004)		Adam *et al*. (1987)		Meyer (1990)		Present work	
E	*I*	*E*	*I*	*E*	*I*	*E*	*I*
748.601 *2*	17.05 *20*	748.603 *8*	17.08 *27*	748.601 *2*	16.94 *19*	748.62 *2*	17.19 *20*
761.22 *6*	0.0156 *19*	761.22 *6*	0.0156 *19*			761.10 *3*	0.017 *1*
776.78 *4*	0.0298 *14*	776.78 *4*	0.0298 *14*			776.59 *5*	0.033 *3*
						783.45 *10*	0.016 *2*
788.876 *12*	15.23 *15*	788.873 *8*	15.32 *26*	788.878	15.12 *18*	788.87 *2*	15.11 *22*
794.7 *3*	0.065 *15*						<0.002
798.92 *3*	0.100 *3*	798.90 *2*	0.104 *3*	798.94 *2*	0.093 *5*	798.90 *2*	0.108 *3*
802.94 *2*	0.089 *3*	802.95 *2*	0.0891 *27*	802.93 *2*	0.088 *5*	802.91 *2*	0.098 *3*
812.634 *10*	0.305 *5*	812.632 *10*	0.305 *5*	812.64 *3*	0.304 *5*	812.62 *2*	0.305 *7*
						842.29 *10*	0.011 *1*
862.863 *15*	0.139 *3*	862.861 *12*	0.1360 *26*	862.86 *3*	0.141 *5*	862.87 *3*	0.135 *2*
875.89 *3*	0.313 *5*	875.943 *10*	0.312 *6*	875.83 *1*	0.313 *5*	875.95 *2*	0.320 *5*
932.96 *5*	1.289 *10*	933.134 *14*	1.31 *4*	932.925 *6*	1.287 *13*	933.13 *2*	1.288 *12*
938.610 *9*	4.96 *6*	938.626 *11*	4.95 *10*	938.605 *5*	4.97 *7*	938.63 *3*	5.03 *4*
947.835 *15*	1.99 *3*	947.873 *10*	1.99 *4*	947.820 *6*	1.97 *4*	947.88 *3*	1.99 *3*
952.68 *3*	0.0220 *9*	952.68 *3*	0.0220 *9*			952.61 *3*	0.0266 *15*
992.204 *4*	0.067 *2*	992.192 *15*	0.0675 *18*	992.205 *4*	0.066 *2*	992.21 *4*	0.066 *2*
1012.610 *21*	0.0466 *14*	1012.61 *2*	0.0466 *14*	1012.59 *5*	0.0465 *15*	1012.61 *4*	0.0514 *11*
1015.31 *3*	0.0252 *10*	1015.31 *3*	0.0252 *10*			1015.25 *9*	0.0260 *24*
1081.58 *3*	0.0376 *14*	1081.58 *3*	0.0382 *14*	1081.58 *6*	0.0362 *15*	1081.57 *3*	0.0356 *27*
1096.67 *5*	0.0033 *3*	1096.59 *8*	0.0035 *3*	1096.70 *5*	0.0029 *5*	1096.79 *12*	0.005 *3*
1207.74 *7*	0.0023 *2*	1207.81 *12*	0.0024 *2*	1207.71 *7*	0.0022 *2*	1207.58 *12*	0.0030 *3*
1220.64 *12*	0.0016 *1*	1220.64 *12*	0.0016 *1*			1220.49 *12*	0.0020 *3*
1231.0 *2*	0.00073 *20*			1231.0 *2*	0.0007 *2*	1231.4 *2*	0.0005 *5*
1246.41 *6*	0.0042 *2*	1246.41 *8*	0.0041 *2*	1246.4 *1*	0.0045 *3*	1246.27 *12*	0.0046 *4*

by providing internal checks on the energy and efficiency calibrations. The samples also contained small amounts of short-lived ^{82}Br (produced from neutron activation of Br which is a contamination in HCl). As the ^{149}Gd decayed, there was a buildup of its daughter ^{149}Eu; typically the initial sample activity included a few percent of ^{149}Eu. A sample γ-ray spectrum from one of the spectroscopy sources is shown in Fig. 2.

Our results have been corrected for detector efficiency as described in Sec. II B. We have also corrected for coincidence summing, as is discussed below. All γ rays identified with ^{149}Gd have been checked for agreement with the expected 9.28-d half-life. In general, our results for the γ-ray energies and intensities are in good agreement with those of previous studies. Exceptions are discussed below. Our discussion of the ^{149}Eu levels is based on the level scheme of the NDS (Ref. [11]). A partial level scheme, relevant to the following discussion of coincidence summing, is shown in Fig. 3.

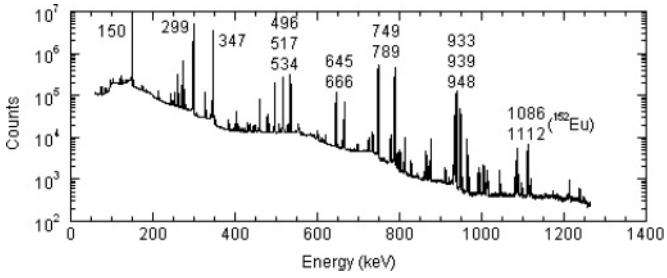

FIG. 2. The γ-ray spectrum from the decay of ^{149}Gd. Prominent peaks are labeled along with two strong peaks from the decay of the ^{152}Eu impurity.

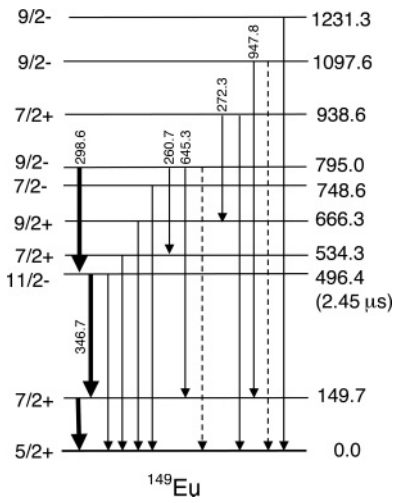

FIG. 3. Partial level scheme of ^{149}Eu as populated in the decay of ^{149}Gd. Dashed lines represent previously reported γ transitions for which we conclude the entire intensity can be ascribed to coincidence summing. The three most intense transitions, shown as bold lines on the left, were used for the cross section determinations.

TABLE III. Coincidence summing in the decay of ^{149}Gd.

Energy (keV)	Coefficient of $(d_{\text{eff}})^{-2}$	Singles intensity (150 keV = 100)	Coefficient of $(d_{\text{eff}})^{-4}$	Coincidence intensity at 5 cm (150 keV = 100)	Summing transitions (keV)
422.06	<0.000001	<0.0003	0.0206(2)	0.106(1)	272.32+149.72
448.37	<0.00001	<0.003	0.0359(3)	0.190(2)	298.63+149.72
496.41	0.0103(1)	3.38(3)	0.160(10)	0.96(6)	346.66+149.72
534.31	0.0188(2)	6.57(7)	<0.016	<0.10	384.54+149.72
645.31	0.0076(1)	3.08(2)	0.0067(67)	0.05(5)	298.63+346.66
666.29	0.00444(2)	1.87(1)	<0.0058	<0.04	516.57+149.72
748.62	0.381(6)	17.49(26)	<0.033	<0.27	598.84+149.72
795.04	<0.000004	<0.002	0.0170(3)	0.147(3)	298.63+496.41
					260.73+534.31
					645.31+149.72
938.63	0.0092(1)	5.00(4)	0.0287(82)	0.28(8)	788.87+149.72
1097.58	<0.000005	<0.004	0.0026(4)	0.029(4)	947.88+149.72
1231.25	0.0000007(7)	0.0005(5)	0.0002(1)	0.0025(12)	1081.57+149.72
					734.85+496.41
					482.66+748.62

1. Coincidence summing

Given that 5 orders of magnitude separate the weakest and strongest transitions in this decay scheme, it is not surprising that coincidence summing plays a significant role in the analysis of the γ-ray intensities. Here we refer only to "true" coincidence summing, that is, two γ rays in cascade from a single nucleus producing a single event in the detector. "Accidental" summing, in which the γ's come from different nuclei, is negligible at the source strengths used in the present work.

It is possible to observe both "summing-in" and "summing-out" effects. In the case of summing-in, γ's of energies E_1 and E_2 produce an event of energy $E_3 = E_1 + E_2$. If the two γ' s are emitted in direct sequence and if there is also a "crossover" transition of energy E_3 emitted, then the summing effect can augment the intensity of E_3. Simultaneously, events of energy E_1 and E_2 are lost from the spectrum, which produces the summing-out effect in those lines.

The singles contribution to the intensity of the line at energy E_3 depends on the detector efficiency at that energy, which is proportional to the inverse square of the effective source-to-detector distance d_{eff}. This effective distance can be approximated by the actual source-to-detector distance plus a correction factor of about half the detector thickness to account for the range of distances over which the incident photons interact in the detector. The summing-in contribution to E_3 depends on the product of the efficiencies for detecting E_1 and E_2; this product is roughly proportional to $(d_{\text{eff}})^{-4}$. The intensity of a peak affected by the summing-in correction should therefore contain a singles contribution proportional to $(d_{\text{eff}})^{-2}$ and a sum coincidence contribution proportional to $(d_{\text{eff}})^{-4}$. The intensity here means the peak areas corrected for counting times and for the source activity but *not* normalized by the 149.7-keV intensity. We can thus represent the variation of any peak intensity I with distance as

$$I = ad_{\text{eff}}^{-2} + bd_{\text{eff}}^{-4}, \tag{2}$$

where the coefficient a is proportional to the true singles intensity and the coefficient b is proportional to the coincidence summing intensity. By fitting our measured intensities to Eq. (2) as a function of distance for nominal distances from 5 to 20 cm, we can obtain the coefficients a and b for various peaks in the spectrum. Table III shows the results of this fit. From the deduced coefficient a for each fit, we have calculated the singles intensity, and then to enable comparison we have normalized the result to the 149.7-keV intensity; this result is shown in the third column of Table III. These deduced normalized intensities differ slightly from the corresponding values in Table II because the fitting process in effect averages unnormalized values and then normalizes them, whereas the values in Table II are first normalized and then averaged (which we feel is the preferable procedure for quoting peak intensities).

For four of the γ's (422.06, 448.37, 795.04, and 1097.58 keV) the entire intensity is due to coincidence summing. That is expected for two of these (422.06 = 272.32 + 149.72, 448.37 = 298.63 + 149.72), because these are "skip-over" cascades in which the γ's are not sequential and, hence, there is no possible γ ray at these energies. In the third case (795.04 keV), three possible sequential cascades can contribute to its intensity (298.63 + 496.41, 260.73 + 534.31, 645.31 + 149.72). It is also possible to have a γ ray of 795.04 keV emitted from the 795.04-keV level to the ground state. Indeed, such a γ has been reported previously [14,15]. According to the presently accepted decay scheme, the 795.04-keV γ would be an M2 transition, which would compete at the 2% level with the 645.31-keV E1 transition from the same level. While not impossible, such competition of M2 with E1 is rare. Our analysis shows that all of the intensity of the 795.04-keV peak can be accounted for through the $(d_{\text{eff}})^{-4}$ term in the distance dependence, and so we conclude that the previously reported 795.04-keV transition is probably a coincidence sum peak.

A similar situation occurs for the 1097.58-keV peak from the level of the same energy. The transition to the ground state would be an M2 transition, which would compete at about the 1% level with the 947.84-keV E1 transition to the first excited state. We were able to observe this peak only in the data at 7.5 and 5 cm. The deduced branching intensity for the 1097.58-keV γ appeared to double as the source was moved from 7.5 to 5 cm, as would be expected for a sum peak.

The 1231.4-keV transition also shows this type of behavior. Because the transition is so weak, we were not able to use the variation in its intensity with distance to eliminate a possible singles component. Our deduced limit for the singles component is in agreement with the intensity reported by Meyer [13].

For some of the transitions listed in Table III (534.31, 645.31, 666.29, and 748.62 keV) the summing effect is negligible in competition with the singles intensity, whereas for others (496.41 and 938.63 keV) the effect must be accounted for. These results agree with calculated values of the coincidence intensity with the exception of 645.31 keV (= 298.63 + 346.66). For this case we expect an effect of about 25% at 5 cm, but we observe an effect of, at most, 3%. A clue to the explanation of this reduction comes from the analysis of the 448.37-keV skip-over transition, in which the observed coincidence peak is only 19% of the expected intensity calculated for 298.63 + 149.72 keV summing. The washing out of the coincidence effect occurs because of the 2.5-μ s lifetime of the 496.39-keV level. Because the 645.31-keV summing cascade proceeds through that same level as intermediate state, we expect a similar reduction in its coincidence summing effect from about 25% to about 5%. The remaining reduction comes about because of the summing-out effects of the component 298.63- and 346.66-keV γ's, which each lose about 4% of their intensity at 5 cm.

2. 132- and 138-keV transitions

Previous results disagree about the relative intensity of these two lines. The NDS [11] and Adam *et al.* [12] put the intensity of 138.10 keV as 15–20% greater than 132.00 keV, while Meyer [13] puts the 132.00-keV intensity as 9% larger than 138.10 keV. Our results clearly show that 132.00 keV has the greater intensity. Furthermore, our spectra show a small well-resolved peak at 139.74 keV. The 139.74-keV peak is possibly also from the decay of ^{149}Gd; the decay of its intensity with time yields a half-life is 8.7±0.5 d, in agreement with the expected 9.28-d half-life. If it is from the ^{149}Gd decay, it could connect the established levels at 938.59 keV (7/2+) and 798.94 keV (9/2−), for which $\Delta E = 139.66$ keV.

3. 214-keV transitions

The peak at 214 keV cannot be fit by a single γ-ray line. This line appears to be an unresolved doublet, with a strong component at the previously identified energy of 214.28 keV and a weaker component whose intensity averaged over all runs amounts to 2.1% of the intensity of the stronger component and whose energy is 0.92 keV below that of the strong component (i.e., 213.36 keV). We were not able to fit the half-life of the weak component directly, but the ratio of the intensities of the two components remained constant to within ±15% over 18 days of running with the sample at two different distances from the detector. It therefore seems possible that this line is associated with the ^{149}Gd decay. The closest match to the present level scheme would be in connecting the 1012.60- and 798.93-keV levels, for which $\Delta E = 213.67$ keV.

4. 418-keV transitions

NDS reports a line at 418.77 ± 0.13 keV, which is assigned as connecting the levels at 952.68 and 534.30 keV ($\Delta E = 418.39$ keV). We see a partially resolved doublet at this energy, with components of 418.35 and 419.47 keV. The former component is in excellent agreement with the expected energy difference for a transition between the 952.68- and 534.40-keV levels. The latter component does not correspond in energy with any of the known impurities in our sample, and its intensity roughly tracks with that of the lower-energy component, suggesting that it is decaying with the same half-life. It is possible that the 419.47-keV γ is a transition in the ^{149}Gd decay, but it does not correspond to any energy difference among the known levels.

5. 436-keV transitions

NDS places two γ's in the decay scheme at the previously measured energy of 436.37 keV. We cannot fit this line as a singlet but do obtain a good fit as an unresolved doublet with energies of 436.24 and 436.62 keV, corresponding respectively to transitions connecting 1231.25 to 795.04 keV ($\Delta E = 436.21$ keV) and 933.11 to 496.39 keV ($\Delta E = 436.72$ keV).

6. 456-keV transition

In agreement with previous work, we have observed a γ ray of energy 456.74 ± 0.04 keV. This γ cannot be fit between any of the known levels of ^{149}Eu. The closest energy-level difference is 456.30 ± 0.02 keV (952.68 to 496.39 keV), but this is too far from statistical agreement with the measured γ-ray energy to be considered a match. Moreover, if our conclusions below concerning the possible 5/2+ assignment to the 952.68-keV level are valid, the 456.30-keV transition would be E3 and thus unlikely to compete so successfully against the M1/E2 transitions from the 952.68-keV level. We conclude that the 456.74-keV transition involves at least one new level not currently identified in the ^{149}Gd decay.

7. 478-keV transitions

The above situation for 436 keV is repeated in the case of 478 keV. We cannot fit this line as a singlet; treating it as a doublet gives an excellent fit with components of 478.27 keV (corresponding to a transition from 1012.60 to 534.30 keV with $\Delta E = 478.30$ keV) and 478.78 keV

(corresponding to a transition from 938.59 to 459.83 keV with $\Delta E = 478.76$ keV).

8. New transitions

In addition to the γ's discussed previously in this report, we observe three new γ's (listed in Table II) that appear to follow the 9.28-d half-life and that can be fit between known levels in ^{149}Eu:

302.58 ± 0.03 keV
(798.94 to 496.39 keV; $\Delta E = 302.55$ keV)
783.45 ± 0.10 keV
(933.11 to 149.73 keV; $\Delta E = 783.38$ keV)
842.29 ± 0.10 keV
(992.21 to 149.73 keV; $\Delta E = 842.48$ keV).

In the absence of coincidence data to verify the placement of these transitions, these assignments should be regarded as tentative.

9. Unobserved γ rays

NDS lists transitions reported by Aleksandrov *et al.* [15] and Vylov *et al.* [16] that were not observed by other investigators. We have searched for evidence of these γ rays in our spectra, and we have been able to place upper limits on their intensities that are in general much smaller than the intensities reported in the previous studies. Table IV lists these transitions and our deduced upper limits. Vylov *et al.* [16] report several "new" transitions that have been previously reported in other works (456.63, 493.11, 776.78, 798.91, 802.96, 952.63, 992.19, and 1015.55 keV). Vylov *et al.* [16] also report transitions of energies 964.25, 1085.92, and 1112.13 keV. We were unable to set upper limits on these three transitions because they fall directly on γ's in our spectra from the decay of the ^{152}Eu impurity. They also report transitions of energies 422.10, 795.00, and 1097.54 keV, which we believe to be sum coincidence peaks, as discussed above. We were not able to either confirm or disprove a line at 842.89 keV (intensity 0.004) reported by Vylov *et al.* [16]. We proposed a new line at 842.29 keV (intensity 0.011), but the energy discrepancy seems too large for these to be the same lines.

A transition of energy 956.4 keV was reported by Cabrera *et al.* [14] (intensity 0.03 ± 0.03) and by Sen *et al.* [17] (intensity 0.035 ± 0.019) but was not reported by other investigators. From our spectra we can set an upper limit of 0.001 on the intensity of a transition at this energy. Because the existence of the 956.4-keV level was proposed on the basis of this transition, we must regard that level as in doubt. No other γ transitions are known to enter or leave this level. If this doubtful level assignment is removed, then the 5/2+ level at 955 ± 3 keV reported in the (p, t) studies [18] could possibly be the level at 952.68 keV populated in the β decay. A 5/2+ assignment would be consistent with the γ transitions definitely assigned to depopulate the 952.68-keV level, and it makes it even more unlikely that the observed 456.74-keV γ ray is associated with the 456.30-keV E3 transition to the 11/2− level at 496.39 keV.

TABLE IV. Upper limits on the intensities of previously reported γ rays in the decay of ^{149}Gd.

Energy (keV)	Previous intensity[a] (150 keV = 100)	Present intensity (150 keV = 100)
127.1	0.02(1)[b]	<0.003
189.7	0.02(1)[b]	<0.005
196.93	0.17(6)	<0.01
203.14	0.09(3)	<0.003
238.25	0.030(5)	<0.003
239.87	0.025(5)	<0.003
248.64	0.032(6)	<0.01
270.79	0.028(12)	<0.01
292.86	0.204(31)	<0.01
372.62	0.03(2)	<0.003
394.59	0.007(2)	<0.002
400.20	0.029(5)	<0.002
429.73	0.08(2)	<0.002
447.42	0.11(3)	<0.01
502.12	0.013(6)	<0.002
522.12	0.006(2)	<0.002
527.92	0.07(3)	<0.003
574.88	0.019(4)	<0.002
577.96	0.005(2)	<0.002
581.79	0.022(9)	<0.002
590.96	0.022(9)	<0.002
593.16	0.014(7)	<0.002
629.01	0.010(4)	<0.001
672.37	0.20(6)	<0.001
688.27	0.025(6)	<0.003
711.72	0.020(8)	<0.001
715.21	0.013(4)	<0.001
719.19	0.023(6)	<0.002
738.66	0.03(1)	<0.002
756.42	0.008(5)	<0.003
872.62	0.012(4)	<0.005
880.04	0.009(4)	<0.002
898.99	0.004(1)	<0.001
956.4	0.035(20)[c]	<0.001

[a]Intensities reported by Vylov *et al.* [16] unless otherwise indicated.
[b]From Aleksandrov *et al.* [15].
[c]From Cabrera *et al.* [14] and Sen *et al.* [17].

Vylov *et al.* [16] propose two new levels in ^{149}Eu: 869.01 and 1050.86 keV. The former is based on their observed γ's at 719.19 and 372.62 keV and the latter on γ's at 590.96 and 238.25 keV. Because we did not observe these γ's, we regard these two levels as doubtful.

IV. CONCLUSIONS

We have determined the radiative neutron capture cross sections of ^{148}Gd to be $\sigma = 9600 \pm 900$ b and $I = 28,200 \pm 2300$ b. It is not unusual to find cross sections in the range of 10^4 b in this region, but for the Gd isotopes the large cross sections were previously observed only for odd-mass isotopes. In that sense our measured values for ^{148}Gd deviate from this systematic behavior. It is not possible to carry the analysis of

the cross sections any further because the neutron resonance structure for ^{148}Gd is not known.

In the decay of ^{149}Gd, we have proposed several new γ transitions (139.74, 302.58, 783.45, and 842.29 keV) on the basis of agreement with the expected half-life and agreement with the expected energy differences between known levels in the ^{149}Eu level scheme. We also propose other new transitions (213.39 and 419.47 keV) and verify an established transition (456.74 keV), none of which can be accommodated within the existing level scheme. We have shown that the intensities of some previously reported peaks can be accounted for as coincidence summing, and we have placed stringent upper limits on the intensities of 34 previously reported peaks. Based on the latter, we conclude that three previously assigned levels (869.01, 956.4, and 1050.86 keV) are doubtful.

ACKNOWLEDGMENTS

We are grateful for the support of the Oregon State University Radiation Center and the staff of the Oregon State TRIGA reactor in enabling these experiments to be carried out. This work was supported in part by the U.S. Department of Energy under contracts DE-FG03-98ER41060 (OSU) and DE-AC03-76SF00098 (LBNL).

[1] S. F. Mughabghab, M. Divadeenam, and N. Holden, *Neutron Cross Sections, Part A, Z = 1−60* (Academic Press, New York, 1981); see also http://www.nndc.bnl.gov

[2] K. S. Krane, M. Rios, R. Ejnisman, I. D. Goldman, R. R. P. Teixeira, Y. Nakazawa, E. B. Norman, and J. Reel, Bull. Am. Phys. Soc. **43**, 1592 (1998).

[3] K. S. Krane, in *Proceedings of the 10th International Symposium on Capture Gamma-Ray Spectroscopy and Related Topics*, edited by Stephen Wender (American Institute of Physics, New York, 2000), p. 111.

[4] http://isotopes.lanl.gov/product.htm

[5] http://www.ipl.isotopeproducts.com

[6] E. Browne and R. B. Firestone, *Table of Radioactive Isotopes* (Wiley & Sons, New York, 1986); see also http://ie.lbl.gov/toi

[7] C. L. Duncan and K. S. Krane, Phys. Rev. C **71**, 054322 (2005).

[8] ORTEC, Inc., http://www.ortec-online.com/pdf/a65.pdf

[9] P. A. Aarnio, J. T. Routti, and J. V. Sandberg, J. Radioanal. Nucl. Chem. **124**, 457 (1988).

[10] K. Debertin and R. G. Helmer, *Gamma- and X-Ray Spectroscopy with Semiconductor Detectors* (North-Holland, Amsterdam, 1988), p. 224.

[11] B. Singh, Nucl. Data Sheets **102**, 1 (2004).

[12] I. Adam, T. Zhelev, D. Zakoucky, B. Kratsik, M. M. Mikhailova, and I. Penev, Izv. Akad. Nauk SSSR, Ser. Fiz. **51**, 2 (1987); Bull. Acad. Sci. USSR, Phys. Ser. (Engl. Transl.) **51**(1), 1 (1987).

[13] R. A. Meyer, Fizika **22**, 153 (1990).

[14] J. A. Cabrera, M. Ortiz, M. Shaw, A. Williart, J. C. Gomez del Campo, and J. Campos, Nucl. Instrum. Methods Phys. Res. A **312**, 364 (1992).

[15] V. S. Aleksandrov, Ts. Vylov, I. I. Gromova, A. A. Klyuchnikov, A. F. Novgorodov, and A. I. Feoktistov, Izv. Akad. Nauk SSSR, Ser. Fiz. **39**, 468 (1975); Bull. Acad. Sci. USSR, Phys. Ser. (Engl. Transl.) **39**(3), 9 (1975).

[16] Ts.. Vylov, Sh. Omanov, O. Kabilov, U. Salikhbaev, and T. Khazratov, Izv. Akad. Nauk, Ser. Fiz. **60**, 176 (1996); Bull. Russ. Acad. Sci. Phys. Ser. (Engl. Transl.) **60**(1), 141 (1996).

[17] P. Sen, H. Bakhru, N. Cue, R. Wiedeman, and J. Sprinkle, Z. Phys. A **275**, 381 (1975).

[18] H. Taketani, H. L. Sharma, and N. M. Hintz, Phys. Rev. C **12**, 108 (1975).